Discrete Variational Xα Studies of the Electronic Structure of Amavadin *

Elaine M. Armstrong,[a] David Collison,[a] Robert J. Deeth [b] and C. David Garner[a]
[a] *Department of Chemistry, The University of Manchester, Manchester M13 9PL, UK*
[b] *Inorganic Computational Group, School of Chemistry, The University of Bath, Claverton Down, Bath BA2 7AY, UK*

Discrete variational Xα (DVXα) calculations have been carried out for the eight-co-ordinated vanadium-(IV) and -(V) complexes $[V(hida)_2]^{2-/1-}$ (H_3hida = *N*-hydroxyiminodiacetic acid). These complexes are minimal models for the corresponding oxidation states of amavadin from *Amanita muscaria* which, as isolated, consists of an approximately equimolar mixture of the anions $[\Delta\text{-}V\{(S,S)\text{-}hidpa\}_2]^{2-}$ and $[\Lambda\text{-}V\{(S,S)\text{-}hidpa\}_2]^{2-}$ (H_3hidpa = *N*-hydroxy-2,2′-iminodipropionic acid). The electronic structure and the nature of the metal-ligand bonding of these vanadium-(IV) and -(V) centres is described. The ordering of the d orbitals and their composition is closely related to that established for the oxovanadium(IV) moiety which demonstrates why, for many years, amavadin was mistakenly thought to contain a VO^{2+} centre.

Vanadium is concentrated by fungi of the *Amanita* genus to remarkably high levels, with the highest concentrations (up to 400 ppm dry weight) being generally found in *Amanita muscaria*.[1] The low molecular weight, blue, vanadium(IV) complex amavadin is readily isolated from *Amanita muscaria*[2] and is constituted as a 1:2 complex of the metal with the pro ligand (*S,S*)-*N*-hydroxy-2,2′-iminodipropionic acid (H_3hidpa). Initially, amavadin was formulated [3,4] as the five-co-ordinated vanadyl complex $[VO(H_2hidpa)_2]$, based on electronic absorption (UV/VIS), electron spin resonance (ESR) and infrared spectroscopic data.[3-8] Amavadin is reversibly oxidized to the vanadium(V) level.[9,10]

An alternative structure for amavadin was proposed, following the synthesis and crystallographic characterisation of $[NH_4][NMe_4][V(hida)_2]$ (H_3hida = *N*-hydroxyiminodiacetic acid).[11] The $[V(hida)_2]^{2-}$ anion involves an eight-co-ordinated vanadium(IV) centre bound by two $hida^{3-}$ ligands, each bonded *via* an η^2-N–O group and two unidentate carboxylato-groups. This arrangement was suggested to apply to amavadin. Our studies [12,13] have shown that this is indeed the case.

Cyclic voltammetric studies of amavadin and its chemical analogues $[V(hida)_2]^{2-}$ and $[V(hidpa)_2]^{2-}$ demonstrate that each of the V^V–V^{IV} pairs possesses a common geometry in solution.[10-13] We have crystallographically characterised six $[V(hidpa)_2]^{n-}$ (n = 1 or 2) complexes and $[V(hida)_2]^-$;[12] Fraústo da Silva and co-workers [11] have reported the structure of $[V(hida)_2]^{2-}$. All of these anions have the co-ordination sphere shown in Fig. 1; the only significant variation within this series of structurally congruent complexes is that the $V\text{–}O_{carboxylate}$ bonds are (on average) 0.1 Å shorter for the vanadium(V) than the vanadium(IV) centres.

We have accomplished [12] an extensive series of spectroscopic studies [X-ray absorption (V^{IV} and V^V); ESR (V^{IV}); ^1H, ^{13}C and ^{51}V NMR (V^V); circular dichroism (V^{IV} and V^V)] for amavadin in its V^{IV} and V^V oxidation states, $[V(hida)_2]^{2-}$ and $[V(hida)_2]^-$, and several variants of $[V(hidpa)_2]^{2-}$ and $[V(hidpa)_2]^-$ with different chiralities at the C^2 carbon and vanadium centres.

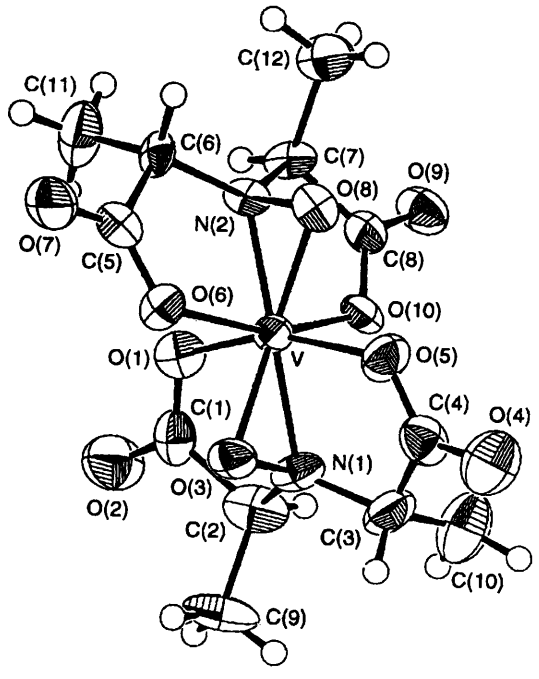

Fig. 1 Structure of the anion of $[PPh_4][\Delta\text{-}V\{(S,S)\text{-}hidpa\}_2]\cdot H_2O$ [12]

These studies showed that amavadin, as isolated, consists of an approximately equal mixture of $[\Delta\text{-}V\{(S,S)\text{-}hidpa\}_2]^{2-}$ and $[\Lambda\text{-}V\{(S,S)\text{-}hidpa\}_2]^{2-}$, each of these anions involving eight-co-ordinated V^{IV} but *no* V=O group (see Fig. 1). The metal–ligand atom distances of amavadin, obtained from an analysis of the vanadium K-edge EXAFS (extended X-ray absorption fine structure) recorded for *Amanita muscaria*,[12,13] are in good agreement with the dimensions obtained from the X-ray crystallographic determinations of the structures of $[V(hida)_2]^{2-}$ [11] and $[V(hidpa)_2]^{2-}$.[12,13] The initial [3,4] assignment of the IR band at 980 cm^{-1} in amavadin to a ν(V=O) stretch was erroneous, rather this band is due to ν(C–Me) stretching.[11] However, amavadin, $[V(hidpa)_2]^{2-}$ and $[V(hida)_2]^{2-}$ do have visible and ESR spectra which resemble those typical of $\{VO\}^{2+}$ complexes. Thus, these anions are blue with three

* *Supplementary data available* (No. SUP 57049, 7 pp.): Molecular orbital energies and compositions for $[V(hida)_2]^{n-}$ (n = 1 or 2). See Instructions for Authors, *J. Chem. Soc., Dalton Trans.*, 1995, Issue 1, pp. xxv–xxx.

Non-SI unit employed: au ≈ 5.29 × 10^{-11} m.

visible absorption bands [typically, λ_{max}/cm^{-1} ($\varepsilon/dm^3\ mol^{-1}\ cm^{-1}$) 12 900(23), 14 300(22), 17 700(25)] and ESR spectra at both X- and Q-band frequencies which are approximately axial (typical parameters $g_{\|} = 1.925$, $g_{\perp} = 1.987$, $A_{\|} = 154 \times 10^{-4}\ cm^{-1}$, $A_{\perp} = 47 \times 10^{-4}\ cm^{-1}$). Therefore, it is necessary to address the question why these eight-co-ordinated *non*-oxo vanadium(IV) complexes have electronic properties, and presumably an electronic structure, similar to those of vanadyl, VO^{2+}, complexes. We have examined this by performing discrete variational (DV) Xα calculations[14] for $[V(hida)_2]^{2-/1-}$. This is a method of calculation which has proved successful in describing the electronic structure of a range of oxo-vanadium(IV) complexes[15] and related oxochromium(V)[16] and oxomolybdenum(V)[17] species.

Experimental

Electronic spectra were recorded on a Shimadzu UV-3101 PC UV/VIS/NIR scanning spectrometer.

Structural Details.—The dimensions of $[V(hida)_2]^{2-}$ and $[V(hida)_2]^-$ have been determined.[11,12] In the solid state, neither of these anions has any point symmetry beyond C_1. However, one bisector of the $O_{carboxylate}$–V–$O_{carboxylate}$ interbond angles closely approximates to a C_2 axis and the atomic positions chosen for the calculations used slightly displaced atomic coordinates to yield idealised (C_2) symmetry. Thus, in Fig. 1, the operation $C_2{}^1$ interchanges the 'top' and 'bottom' ligands and hence the two V–O–N triangles.

Computational Details.—The density functional theorem provides a rigorous basis for the *exact* calculation of the ground-state electron density of any molecule.[18] Such a treatment would include *all* possible electron exchange/correlation interactions. Unfortunately, the theorem merely proves that such an exact functional exists, not how to generate it. Practical computational procedures therefore employ approximations to this hypothetical exact functional. One such scheme is the DVXα model. The Xα methods employ only the exchange part of the full local density approximation (LDA) functional. The absence of a correlation term is partially compensated by using an α factor of 0.7 rather than the formal LDA value of 2/3. The discrete variational implementation is the forerunner of the DMol program system.[19,†] It is a numerical scheme which we have shown on several occasions[15–17,20,21] to give accurate electronic spectral properties for a range of d^1 and d^9 metal complexes. The method has been described in detail elsewhere[14,20] although some relevant points are repeated here.

Self-consistent charge[22] (SCC) DVXα calculations have been carried out for $[V(hida)_2]^{2-/1-}$ within a spin-restricted formalism. Near-minimal single site orbital (SSO) basis sets[23] (or numerical atomic orbitals, NAOs) were employed (up to 4p on V, up to 2p on O, N and C and 1s on H) with the core functions (up to 3p on V, 1s on O, C and N) frozen[24] and orthogonalised against the valence orbitals. The SSO basis sets, which are of approximately double-ζ quality,[25] were further constrained by applying an external potential well of depth −2 au, with inner and outer radii of 4 and 6 au for V and 2 and 4 au, respectively, for O, C, N and H. The basis sets were optimised as previously described.[20]

Sampling points were distributed such that *ca.* 1100 points were associated with V, 500–600 points with C, N and O and 300 points with H. This distribution scheme ensures a numerical error of approximately ± 0.02 eV (*ca.* 3.20×10^{-21} J) in molecular orbital energies and ± 0.002 in atomic orbital populations, relative to the limit of a very large number of sampling points.

All charge densities and orbital populations are based on Mulliken analyses.[26] Estimates of both d–d and charge transfer (c.t.) transition energies were computed using Slater's transition-state formalism.[27] In this latter procedure, a calculation is performed using molecular-orbital (MO) occupations corresponding to the halfway point in the transition. Transition-state data are generally in better agreement with experiment than Xα MO energy differences, particularly if significant electronic relaxation accompanies the excitation. Full listings of MO energies and compositions for $[V(hida)_2]^{n-}$, where $n = 1$ or 2, are available as SUP 57049.

† DMol is available from Biosym Technologies, San Diego, CA.

Results and Discussion

The sequence of '3d orbital' energies calculated for $[V(hida)_2]^{2-}$ is $d_{x^2-y^2} < d_{yz} < d_{xz} < d_{xy} < d_{z^2}$, see Fig. 2 and Table 1 which also lists the percentage d character of these levels. Thus, the singly occupied molecular orbital (SOMO) of $[V(hida)_2]^{2-}$ has substantial (82%) d character, is metal–ligand non-bonding, and is directed between the carboxylate oxygen atoms along the *x*- and *y*-axes (Fig. 2). The V–$O_{carboxylate}$ σ* orbital is predominantly d_{xy} in character. The d_{yz}, d_{xz} and d_{z^2} orbitals are used to form bonds to the two 'axial' η^2-N-O groups. Fig. 3 shows the distribution contours for the π* MO involving $3d_{xz}$ and Fig. 4 the distribution contours for the σ* MO involving $3d_{z^2}$. The d_{yz} and d_{xz} orbitals are not degenerate, but are split by some 900 cm^{-1} since the $O_{carboxylate}$–V–$O_{carboxylate}$ in-plane interbond angles are not exactly 90° and the two η^2-N–O groups are not perfectly staggered in projection down the *z* axis.[11,12] The overall relative ordering of the d orbitals (Table 1, Fig. 2) shows that the d_{yz}, d_{xz} 'pair' are *ca.* 4000 cm^{-1} to lower energy than d_{xy} which, in turn, is only *ca.* 1000 cm^{-1} below the energy of the d_{z^2} orbital. The computed d–d band energies are in good agreement with the observed values for $[V(hida)_2]^{2-}$,

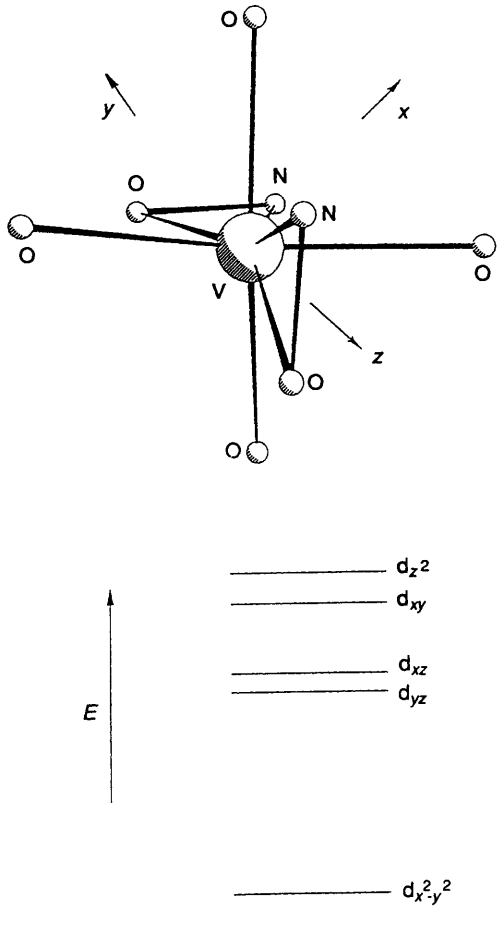

Fig. 2 Idealised co-ordination geometry and qualitative d-orbital splitting diagram for $[V(hida)_2]^{2-}$, $[V(hidpa)_2]^{2-}$ and amavadin

Table 1 DVXα computed d-orbital sequences and percentage d character

Complex	d-Orbital sequence
$[VOCl_4]^{2-}$*	$d_{x^2-y^2} < d_{xy} < d_{xz},d_{yz} < d_{z^2}$
%d	88.6 72.7 72.0 57.5
$[V(hida)_2]^{2-}$	$d_{x^2-y^2} < d_{yz} < d_{xz} < d_{xy} < d_{z^2}$
%d	81.6 66.9 63.4 75.4 66.7
$[V(hida)_2]^-$	$d_{x^2-y^2} < d_{yz} < d_{xz} < d_{z^2} < d_{xy}$
%d	74.6 62.1 58.7 73.6 72.7

* From ref. 15 with the *x*- and *y*-axes rotated by 45°.

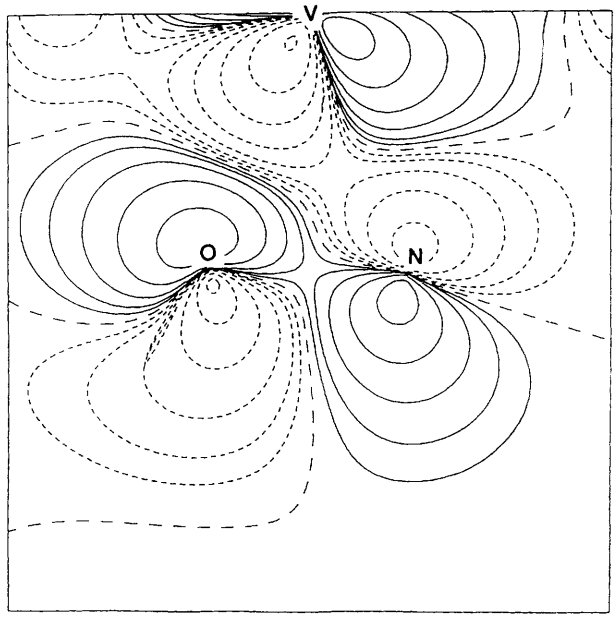

Fig. 3 Distribution contours for the π* MO (31a) with predominant d_{xz} N, O character in $[V(hida)_2]^{2-}$, viewed perpendicular to one V–NO plane with only the -*z* portion shown

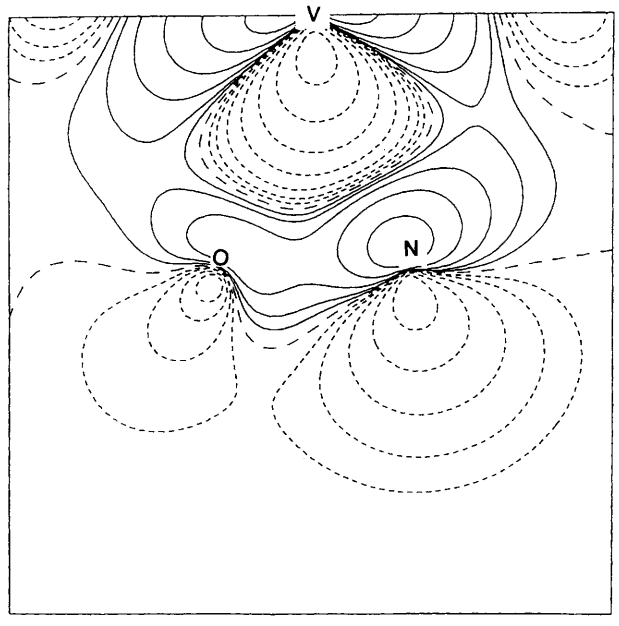

Fig. 4 Distribution contours for the σ* MO (32a) with predominant d_{z^2} N, O character in $[V(hida)_2]^{2-}$, viewed perpendicular to one V–NO plane with only the -*z* portion shown

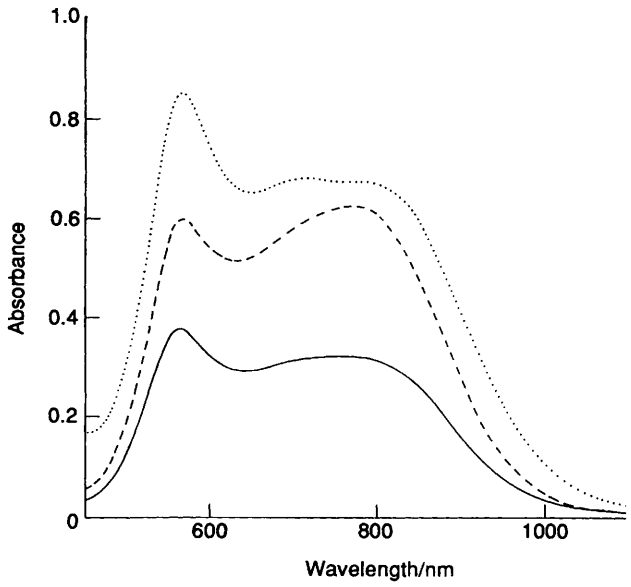

Fig. 5 Electronic spectra of $[NH_4][NMe_4][V(hida)_2]$ (26.7 mmol dm^{-3}) in H_2O (• • •); amavadin (29.3 mmol dm^{-3}) in aqueous 0.2 mol dm^{-3} phosphate buffer, pH 5.8 (- - -); and $H_2[V(hidpa)_2]\cdot 3H_2O$ (14.4 mmol dm^{-3}) in H_2O (—)

$[V(hidpa)_2]^{2-}$ and amavadin (Table 2). The prediction of four d–d transitions in the region 11 500–18 000 cm^{-1} is consistent with the three λ_{max} observed (Fig. 5) in this region, since the $d_{x^2-y^2} \longrightarrow d_{yz}$ and $\longrightarrow d_{xz}$ transitions are predicted to be close (< 1000 cm^{-1}) in energy and would not be expected to be resolved by these measurements. The largest discrepancy is *ca.* 1700 cm^{-1} for the $d_{x^2-y^2} \longrightarrow d_{xy}$ transition, the λ_{max} of which is the most difficult to define (Fig. 5). The onset of charge-transfer (c.t.) bands observed at *ca.* 22 500 cm^{-1} agrees well with the calculated value at *ca.* 24 000 cm^{-1} (Table 3).

Oxidation from $[V(hida)_2]^{2-}$ to $[V(hida)_2]^-$ results in the calculated d-orbital sequence changing only in that the two highest energy orbitals, d_{xy} and d_{z^2}, are reversed. Thus for vanadium(v) the σ-bonding effect of the four carboxylate oxygens on the 'in-plane' orbital is dominant. This is expected, as the removal of the single (unpaired) electron from this plane on oxidation leads to a concomitant reduction of *ca.* 0.1 Å in $V–O_{carboxylate}$ bond lengths. The electronic absorption spectrum of $[V(hida)_2]^-$ is dominated by a band at 20 800 cm^{-1}; the computed transition energies show that this band may arise from carboxylate $\longrightarrow$ vanadium and/or $O_{N-O} \longrightarrow$ vanadium transitions. These c.t. transitions are *ca.* 4500 cm^{-1} *lower* in energy for $[V(hida)_2]^-$ as compared with $[V(hida)_2]^{2-}$ (Table 3). The electronic absorption spectra of $[V(hidpa)_2]^-$ and oxidised amavadin are essentially the same and very similar to that of $[V(hida)_2]^-$.

Thus, the electronic structure of all members of this family of eight-co-ordinated vanadium complexes can be described by the basis derived for the $[V(hida)_2]^{2-/1-}$ derivatives.

The d-orbital sequences given in Table 1 show that there is a considerable similarity between $[V(hida)_2]^{2-}$ and $[VOCl_4]^{2-}$. The SOMO in both cases [15] has substantial d-electron character and is predominantly located in a 'non-bonding' orbital pointing between the 'in-plane' ligands. The axial bonding in both cases involves d_{yz}, d_{xz} (π) and d_{z^2} (σ) interactions, with the former two d orbitals being at a lower energy than the last. The 'in-plane' σ-antibonding orbital is predominantly d_{xy} in character and is at a higher energy relative to the SOMO for $[V(hida)_2]^{2-}$ than $[VOCl_4]^{2-}$, as would be expected when the relative interactions (ligand-field strengths) of O- and Cl-donor ligands are compared.

The nature of the metal–ligand bonding in $[V(hida)_2]^{2-}$ and $[VOCl_4]^{2-}$ can be probed *via* a Mulliken analysis of the ground

Table 2 Comparison of the d–d band energies (cm^{-1}) calculated for $[V(hida)_2]^{2-}$ with those observed for $[V(hida)_2]^{2-}$, $[V(hidpa)_2]^{2-}$ and amavadin

	$[V(hida)_2]^{2-a}$		$[V(hidpa)_2]^{2-b}$	Amavadin[c]
	Calculated	Observed (ε/dm^3 mol^{-1} cm^{-1})	Observed (ε/dm^3 mol^{-1} cm^{-1})	Observed (ε/dm^3 mol^{-1} cm^{-1})
$d_{x^2-y^2} \longrightarrow d_{yz}$	11 556	12 500 (25.1)	13 175 (22.1)	12 950 (21.3)
$d_{x^2-y^2} \longrightarrow d_{xz}$	12 431			
$d_{x^2-y^2} \longrightarrow d_{xy}$	16 002	14 170 (25.5)	14 330 (21.6)	14 470 (19.5)
$d_{x^2-y^2} \longrightarrow d_{z^2}$	17 085	17 760 (31.7)	17 760 (23.4)	17 670 (20.5)

[a] $[NH_4][NMe_4][V(hida)_2]$ in H_2O. [b] $H_2[V(hidpa)_2]$ in H_2O. [c] Aqueous 0.2 mol dm^{-3} phosphate buffer (pH 5.8).

Table 3 Computed metal-to-ligand (m.l.) and ligand-to-metal (l.m.) charge-transfer (c.t.) transition energies (cm^{-1})*

$[V^{IV}(hida)_2]^{2-}$		$[V^{V}(hida)_2]^{-}$	
m.l.c.t.		l.m.c.t.	
30a ⟶ 32b ($V \longrightarrow CO_2^-$)	24 313	29b ⟶ 30a ($CO_2^- \longrightarrow V$)	23 866
30a ⟶ 33a ($V \longrightarrow CO_2^-$)	24 775	29a ⟶ 30a ($CO_2^- \longrightarrow V$)	25 132
30a ⟶ 33b ($V \longrightarrow CO_2^-$)	27 691	28a ⟶ 30a ($O_{N,O} \longrightarrow V$)	25 504
30a ⟶ 34a ($V \longrightarrow CO_2^-$)	27 691	28b ⟶ 30a ($CO_2^- \longrightarrow V$)	26 769
		27b ⟶ 30a ($O_{N,O} \longrightarrow V$)	27 531
		27a ⟶ 30a ($CO_2^- \longrightarrow V$)	28 160
l.m.c.t.			
29a ⟶ 30a ($O_{N,O} \longrightarrow V$)	29 976		
29b ⟶ 30a ($CO_2^- \longrightarrow V$)	29 517		

* All other c.t. band energies > 30 000 cm^{-1}.

Table 4 DVXα calculated atomic charges and overlap populations per ligand for $[V(hida)_2]^{2-}$ and $[VOCl_4]^{2-}$

Atomic charges			
	$[V(hida)_2]^{2-}$		$[VOCl_4]^{2-}$
V	1.011		0.977
L_{ax}	−0.374		−0.483
L_{eq}	−0.603		−0.624
Overlap populations per ligand			
	$[V(hida)_2]^{2-}$		$[VOCl_4]^{2-}$
V–(NO)	0.644	V=O	0.913
$V-O_{eq}$	0.325	V–Cl	0.346

state and the calculated charge density and the atomic charges are listed in Table 4. For $[V(hida)_2]^{2-}$, the calculated atomic charge for the metal, 1.011, is significantly lower than the formal oxidation state of IV. This effect was also observed for oxovanadium(IV) complexes[15] and the value for $[V(hida)_2]^{2-}$ is between the values calculated for $[VOCl_4]^{2-}$ (0.977) and $[VO(NCS)_4(H_2O)]^{2-}$ (1.042). The calculated atomic charge on the carboxylate ligand atoms of $[V(hida)_2]^{2-}$ of −0.603 is comparable to that calculated for chloride (−0.624) and thiocyanate (−0.688) in the above oxovanadium(IV) complexes. For $[V(hida)_2]^{2-}$, the charge associated with *each* 'axial' η^2-N–O ligand is −0.374, as compared with −0.483 for the total charge on the oxo-group in $[VOCl_4]^{2-}$. Previous studies[15,28,29] have shown that the large donation from a vanadyl oxygen atom is consistent with strong, formally multiple V=O bonding. Whilst each 'axial' component in $[V(hida)_2]^{2-}$ is not quite as strong a donor as O^{2-}, there are *two* η^2-N–O moieties compared to *one* oxo group. Although total charge and spin densities allow for some comparison between complexes, the use of these quantities is not completely satisfactory. A comparison of the bonding properties of disparate ligands can be more effectively achieved through the use of overlap populations.[15–17] Although it has been clearly demonstrated that the bonding in vanadium(IV) complexes must be dealt with on an individual basis,[15] the comparison between $[V(hida)_2]^{2-}$ and $[VOCl_4]^{2-}$ is, nonetheless, informative. The $V-O_{carboxylate}$ and V–Cl overlap populations are similar (Table 4), being 0.325 and 0.346, respectively. The large overlap population for the vanadyl species (0.913) is consistent with considerable covalent bonding. The equivalent value for each η^2-N–O group is 0.644, which is larger than any overlap population computed previously[15] for a ligand other than an oxo group to vanadium(IV), *viz.* equatorial CN in $[VO(CN)_5]^{3-}$ is 0.628. Since there is a pair of *trans*-η^2-N–O groups, the overlap population is consistent with a very strong axial ligand field in $[V(hida)_2]^{2-}$ and related complexes.

Conclusion

Discrete variational Xα calculations on $[V(hida)_2]^{2-/1-}$ have demonstrated that the energies and compositions of the orbitals with a predominant d character are very similar to those found for oxovanadium(IV) complexes and this is in accordance with the qualitative considerations of crystal-field theory.[30] This observation demonstrates how amavadin could have been mistaken for a vanadyl, $\{VO\}^{2+}$, species on the basis of electronic absorption and ESR spectroscopy. The similarity of bonding of one oxo-group to two *trans* η^2-N–O groups has also been observed in respect to the redox sequences $[Mo(hidpa)_2]^{2-} \longleftrightarrow [Mo(hidpa)_2]^{-} \longleftrightarrow [Mo(hidpa)_2]$ and $\{MoO\}^{2+} \longleftrightarrow \{MoO\}^{+} \longleftrightarrow \{MoO\}$.[31]

The results reported herein further demonstrate that the DVXα method is sufficiently accurate to provide useful information concerning the electronic structure of complex molecules.

Acknowledgements

We acknowledge The Royal Society for financial support (to D. C., R. J. D.); R. J. D. thanks Professor D. E. Ellis (Northwestern University, Chicago) for making his DVXα software available and Sun Microsystems Computer Corporation and the Science and Engineering Research Council Computational Science Initiative for the provision of computer hardware.

References

1 H.-U. Meisch, W. Reinle and J. A. Schmitt, *Naturwissenschaften*, 1979, **66**, 620.
2 E. Bayer and H. Kneifel, *Z. Naturforsch., Teil B*, 1972, **27**, 207.
3 H. Kneifel and E. Bayer, *Angew. Chem., Int. Ed. Engl.*, 1973, **12**, 508.
4 H. Kneifel and E. Bayer, *J. Am. Chem. Soc.*, 1986, **108**, 3075.
5 J. Felcman and J. J. R. Fraústo da Silva, *Talanta*, 1983, **30**, 565.
6 R. D. Gillard and R. J. Lancashire, *Phytochemistry*, 1983, **23**, 179.
7 P. Krauss, E. Bayer and H. Kneifel, *Z. Naturforsch., Teil B*, 1984, **39**, 829.
8 E. Koch, H. Kneifel and E. Bayer, *Z. Naturforsch., Teil C*, 1987, **42**, 873.
9 M. A. Nawi and J. L. Riechel, *Inorg. Chim. Acta*, 1987, **136**, 33.
10 J. J. R. Fraústo da Silva, *Chem. Spec. Bioavail.*, 1989, **1**, 139.
11 M. A. A. F. de C. T. Carrondo, M. T. L. S. Duarte, J. C. Pessoa, J. A. L. Silva, J. J. R. Fraústo da Silva, M. C. T. A. Vaz and L. F. Vilas-Boas, *J. Chem. Soc., Chem. Commun.*, 1988, 1158.
12 E. M. Armstrong, R. L. Beddoes, L. J. Calviou, J. M. Charnock, D. Collison, N. Ertok, J. H. Naismith and C. D. Garner, *J. Am. Chem. Soc.*, 1993, **115**, 807.
13 E. M. Armstrong, M. S. Austerberry, R. L. Beddoes, D. Collison, J. M. Charnock, S. N. Ertok, C. D. Garner and M. Helliwell, unpublished work.
14 D. E. Ellis and G. S. Painter, *Phys. Rev. B*, 1970, **2**, 2887.
15 R. J. Deeth, *J. Chem. Soc., Dalton Trans.*, 1991, 1467.
16 R. J. Deeth, *J. Chem. Soc., Dalton Trans.*, 1990, 365.
17 R. J. Deeth, *J. Chem. Soc., Dalton Trans.*, 1991, 1895.
18 T. Ziegler, *Chem. Rev.*, 1991, **91**, 651.
19 E. Wimmer, A. Freeman, C.-L. Fu, S.-H. Cao and B. Delley, *ACS Symp. Ser.*, 1987, **353**, 49.
20 R. J. Deeth, *J. Chem. Soc., Dalton Trans.*, 1990, 355.
21 R. J. Deeth, B. N. Figgis and M. I. Ogden, *Chem. Phys.*, 1988, **121**, 115.
22 A. Rosen, D. E. Ellis, H. Adachi and F. W. Averill, *J. Chem. Phys.*, 1976, **65**, 3629.
23 B. Delley and D. E. Ellis, *J. Chem. Phys.*, 1982, **76**, 1949.
24 E. J. Baerends, D. E. Ellis and P. Ros, *Chem. Phys.*, 1973, **2**, 41.
25 F. W. Averill and D. E. Ellis, *J. Chem. Phys.*, 1973, **59**, 6412.
26 R. S. Mulliken, *J. Chem. Phys.*, 1955, **23**, 1833, 1841.
27 J. C. Slater, *Quantum Theory of Molecules and Solids*, McGraw-Hill, New York, 1974, vol. 4.
28 C. J. Ballhausen and H. B. Gray, *Inorg. Chem.*, 1962, **1**, 111.
29 D. Collison, B. Gahan, C. D. Garner and F. E. Mabbs, *J. Chem. Soc., Dalton Trans.*, 1980, 667.
30 D. Collison. *J. Inorg. Biochem.*, 1991, **43**, 403.
31 H. S. Yadav, E. M. Armstrong, R. L. Beddoes, D. Collison and C. D. Garner, *J. Chem. Soc., Chem. Commun.*, 1994, 605.

Received 21*st July* 1994; *Paper* 4/04462B